



Innate Response Activator B Cells Protect Against Microbial Sepsis

Citation

Rauch, P. J., A. Chudnovskiy, C. S. Robbins, G. F. Weber, M. Etzrodt, I. Hilgendorf, E. Tiglao, et al. 2012. "Innate Response Activator B Cells Protect Against Microbial Sepsis." *Science* 335 (6068): 597–601. <https://doi.org/10.1126/science.1215173>.

Permanent link

<http://nrs.harvard.edu/urn-3:HUL.InstRepos:41384252>

Terms of Use

This article was downloaded from Harvard University's DASH repository, and is made available under the terms and conditions applicable to Other Posted Material, as set forth at <http://nrs.harvard.edu/urn-3:HUL.InstRepos:dash.current.terms-of-use#LAA>

Share Your Story

The Harvard community has made this article openly available.
Please share how this access benefits you. [Submit a story](#).

[Accessibility](#)



Published in final edited form as:

Science. 2012 February 3; 335(6068): 597–601. doi:10.1126/science.1215173.

Innate Response Activator B Cells Protect Against Microbial Sepsis

Philipp J. Rauch^{1,*}, Aleksey Chudnovskiy^{1,*}, Clinton S. Robbins^{1,†,*}, Georg F. Weber¹, Martin Etzrodt¹, Ingo Hilgendorf^{1,5}, Elizabeth Tiglao¹, Jose-Luiz Figueiredo¹, Yoshiko Iwamoto¹, Igor Theurl^{1,6}, Rostic Gorbatov¹, Michael T. Waring³, Adam T. Chicoine³, Majd Mouded⁴, Mikael J. Pittet¹, Matthias Nahrendorf¹, Ralph Weissleder^{1,2}, and Filip K. Swirski^{1,†}

¹Center for Systems Biology, Massachusetts General Hospital and Harvard Medical School, Boston, MA 02114, USA

²Department of Systems Biology, Harvard Medical School, Boston, MA 02115, USA

³Ragon Institute Imaging Core, Massachusetts General Hospital and Harvard Medical School, Boston, MA 02114, USA

⁴Division of Pulmonary, Allergy, and Critical Care Medicine, University of Pittsburgh School of Medicine, Pittsburgh, PA 15213, USA

⁵Department of Cardiology, University Hospital Freiburg, 79106 Freiburg, Germany

⁶Department of General Internal Medicine, Clinical Immunology and Infectious Diseases, University Hospital of Innsbruck, A-6020, Innsbruck, Austria

Abstract

Recognition and clearance of bacterial infection is a fundamental property of innate immunity. Here we describe an effector B cell population that protects against microbial sepsis. Innate response activator (IRA)-B cells are phenotypically and functionally distinct, develop and diverge from B1a B cells, depend on pattern recognition receptors, and produce GM-CSF. Specific deletion of IRA-B cell activity impairs bacterial clearance, elicits a cytokine storm, and precipitates septic shock. These observations enrich our understanding of innate immunity, position IRA-B cells as gatekeepers of bacterial infection, and identify new treatment avenues for infectious diseases.

Sepsis is characterized by whole-body inflammation to overwhelming infection (1). Over the last thirty years, sepsis' incidence has risen, indicating a need for a better understanding of its complex pathophysiology (2, 3). The growth factor granulocyte macrophage colony stimulating factor (GM-CSF) elicits multiple changes in cells expressing its cognate receptor. Yet, despite GM-CSF's multiple functions and known relationship with innate leukocytes, its *in vivo* cellular source and role in sepsis remain uncertain (4).

[†]To whom correspondence should be addressed. fswirski@mgh.harvard.edu (F.K.S.); robbins.clinton@mgh.harvard.edu (C.S.R.).

*These authors contributed equally to this work.

Supporting Online Material

www.sciencemag.org/cgi/content/full/science.1215173/DC1

Materials and Methods

Figs. S1 to S12

Table S1

References (29–36)

Profiling of GM-CSF expression by flow cytometry led to a surprising observation. Among the organs, the bone marrow and spleen contained the majority of GM-CSF⁺ cells in the steady state ($1.0 \pm 0.1 \times 10^6$ and $2.9 \pm 0.8 \times 10^5$ cells, respectively) (Fig. 1A) (5). In response to lipopolysaccharide (LPS), a component of gram negative bacteria, GM-CSF⁺ cells increased in number preferentially in the spleen ($3.2 \pm 0.2 \times 10^6$ cells), and were predominantly B220⁺ MHCII⁺ CD19⁺ IgM⁺ B cells (Fig. 1B and fig. S1, A and B). This is surprising because GM-CSF is believed to be produced *in vivo* by non-hematopoietic cells, macrophages, and, in some cases, T cells (4, 6). Nevertheless, B cells constituted the largest GM-CSF⁺ population under these conditions (fig. S1C), a finding that we confirmed by Western blot analysis (Fig. 1C). We named these B cells innate response activator (IRA) B cells because of GM-CSF's known role in activating innate leukocytes. Numerous IRA-B cells accumulated in the spleen in a mouse model of sepsis (fig. S2, A and B) (7) and in response to *Escherichia coli* infection (fig. S2C), indicating that IRA-B cell expansion is a general feature of the body's response to bacteria. In humans, we detected CD19⁺ CD20⁺ IRA-B cells expressing varying levels of CD43, CD27 (fig. S2, D and E), and CD284 (TLR4) (fig. S2F) (8). We therefore elected to characterize murine IRA-B cells in more detail.

Immunofluorescence of spleen sections from LPS recipients co-localized the GM-CSF signal with round mononuclear cells expressing IgM, B220, PAX5, and CD19 (Fig. 1D and fig. S1D) in the red pulp (Fig. 1, E and F). RT-PCR experiments conducted on sorted cells and unprocessed tissue from wild type or B cell-deficient μ MT mice indicated that B cells produce GM-CSF (Fig. 1G). Serum GM-CSF levels were negligible (i.e., below the 7.8 pg/ml detection limit of the assay), a finding that is consistent with the observation that GM-CSF is rapidly removed through receptor-mediated clearance (9). Collectively, these data indicate that inflammation expands the IRA-B cell population *in vivo*.

B cells are linked developmentally, reside in different regions, and mediate distinct functions (10–14). We profiled IRA-B cells according to several well-established methods (13, 15, 16). Our experiments revealed that (CD19⁺ B220⁺ MHCII⁺ GM-CSF⁺) IRA-B cells are phenotypically unique. They are: IgM^{high} CD23^{low} CD43^{high} CD93⁺ (Fig. 2, A and B, and fig. S3A); IgD^{low} CD21^{low} (fig. S3B); CD138⁺ VLA4^{high} LFA1^{high} CD284⁺ (Fig. 2C and fig. S3, C and D); and CD5^{int} (fig. S3, E and F). IRA-B cells contained large stores of intracellular IgM (fig. S4A) and spontaneously secreted IgM, but not IgA or IgG₁ (fig. S4, B and C). In addition to GM-CSF, IRA-B cells produced IL-3 but not pro-IL-1 β , IL-6, and TNF α (fig. S4D). We failed to detect IL-10 expression by IRA-B cells in any of the conditions. Thus, IRA-B cells have a unique B cell phenotype and are functionally distinct from other B cells, including the recently described IL-10-producing B10 B cells (17).

The ability to sort IRA-B cells according to their surface phenotype (fig. S5A) allowed us to profile their transcriptome. Unsupervised hierarchical clustering (Fig. 2D) and principal component analysis (PCA) (Fig. 2E) grouped IRA-B cells in a separate population from T1, FO, MZ, B1a and PC. IRA-B cells also gave rise to a unique transcriptome signature (fig. S5, B to D, and table S1), and expressed genes relevant to B cell biology (fig. S5D).

To decipher where IRA-B cells fit in the B cell lineage we performed several parabiosis and fate-mapping studies. First, we reasoned that if IRA-B cells derive from a circulating precursor they should have high chimerism in a parabiosis setting. Joining CD45.1⁺ with CD45.2⁺ mice revealed high chimerism among IRA-B cells (Fig. 3A), T1 and FO B cells (fig. S6A), but markedly lower chimerism for the spleen-resident MZ B cells and their precursors (fig. S6A). Thus, IRA-B cells derive from a circulating cell.

Second, to identify the IRA-B cell precursor, we adoptively transferred B cell subsets to mice receiving LPS for 3 days (fig. S6, B to E). Among the subsets (splenic T1, FO, MZ, B1 and peritoneal B1a, B1b, B2) only peritoneal B1 B cells (Fig. 3B) gave rise to IRA-B cells. Of these, B1a B cells were the dominant precursor. B1a-derived IRA-B cells readily proliferated (fig. S6E), and developed in the spleen after relocating from the peritoneum (fig. S7). These findings confirm that B1a B cells travel to the spleen in response to peritoneal TLR stimuli (18, 19), and indicate that, upon splenic accumulation, B1a B cells can differentiate to IRA-B cells.

The ontogenic relationship between B1a and IRA-B cells raised the question whether IRA-B cells constitute a distinct subset. To elucidate this, we first placed peritoneal B1a B cells in culture. In response to LPS, B1a B cells separated into three discrete populations: CD138⁻ cells resembling “unchanged” B1a B cells, and two populations of CD138⁺ cells, IRA-B cells among them (fig. S8A). In vitro, IRA-B cells spontaneously secreted GM-CSF (fig. S8B). Second, we sorted peritoneal B1a B cells, IRA-B cells, and splenic CD43⁺ CD138⁺ cells, and followed their fate in vivo. B1a B cells gave rise to multiple cell types (fig. S9A), including IRA-B and CD43⁺CD138⁺ cells, whereas (CD43^{high} CD138⁺) IRA-B and CD43⁺ CD138⁺ cells remained phenotypically segregated (fig. S9, B and C). The data suggest that B1a B cells give rise to distinct cells. IRA-B cells are a subset of this group.

Surface phenotype and fate-mapping studies, though important, reveal little about function. How IRA-B cells arise was our next question. Expectedly, B cell-deficient μ MT (20) and *Cd19*^{-/-} (21) mice did not develop IRA-B cells (Fig. 3, C and D). Surprisingly, *Tnfrsf13c*^{-/-} mice lacking the B-cell activating factor receptor (BAFFR) failed to generate IRA-B cells; BAFFR is believed to be dispensable to B1 B cells (22). At the level of microbial recognition, mice lacking the LPS receptor TLR4 or its adaptor MyD88, but not TRIF, did not generate IRA-B cells (Fig. 3, C and D), indicating a specific MyD88-dependent pathway. The process could depend on direct B1a binding to LPS via TLR4, or on indirect, extrinsic factors such as TLR4-expressing macrophages. To discriminate between these two possibilities, we adoptively transferred B1a B cells from wt mice into *Tlr4*^{-/-} mice (Fig. 3E). B1a wt B cells, but not endogenous *Tlr4*^{-/-} B cells, differentiated to IRA-B cells, indicating that direct TLR4 signaling on B1a B cells is sufficient to generate IRA-B cells.

To test whether IRA-B cells are restricted to TLR4-mediated recognition, we injected TLR ligands Pam3CSK4 (ligand for TLR1/2), Poly(I:C) (TLR3), FLA-ST (TLR5), FSL-1 (TLR2/6), R848 (TLR7/8), and CpG ODN1668 (TLR9). The ligands Pam3CSK4, FSL-1 and R848 yielded IRA-B cells (fig. S10A), a finding that we confirmed in vitro (fig. S10B). We also wondered whether GM-CSF can play an autocrine role for B1a-IRA-B cell conversion (23). B1a cells expressed *Csf2R β* (CD131) (fig. S11A) and, when placed in culture with antibodies against CD131, failed to give rise to IRA-B cells (fig. S11, B and C), but remained alive and gave rise to CD43⁺ CD138⁺ cells. Thus, IRA-B cells develop via MyD88-dependent pathways and use GM-CSF as an autocrine factor.

The spleen's open circulation (24) allows blood leukocytes to enter and exit easily. To reside in the spleen, leukocytes resort to adhesive ligands; MZ B cells, for example, rely on VLA-4 and LFA-1 (25). We wondered whether splenic IRA-B cells, which express VLA-4 and LFA-1 at high levels, might behave similarly. Injection of neutralizing antibodies to VLA-4 and LFA-1 diminished IRA-B cell numbers, revealing that, indeed, the two integrins are responsible for retention (Fig. 3F).

Are IRA-B cells functionally important? To answer this, we focused on the cecal ligation and puncture (CLP) sepsis model (26). We generated mixed chimeras by reconstituting lethally irradiated mice with μ MT and GM-CSF-deficient (*Csf2*^{-/-}) bone marrow cells. In

these mice (called GM/ μ MT chimeras), the μ MT marrow contributed all leukocytes except B cells whereas the *Csf2*^{-/-} marrow contributed only *Csf2*^{-/-} cells. Consequently, the only population completely lacking the capacity to produce GM-CSF in the reconstituted mice were B cells. We tested the quality of the chimeras and their controls by PCR (fig. S11, A and B) and by flow cytometry (fig. S11, C and D).

In response to severe CLP, 40% of control mice survived and recovered, but every GM/ μ MT chimera died within 2 days (Fig. 4, A and B). To characterize this phenotype further, we profiled GM/ μ MT chimeras and controls for several sepsis-relevant indices 20 hours after CLP, prior to any mortalities. Compared to IRA-B cell-containing controls (fig. S11E), the peritoneal cavity of GM/ μ MT chimeras had more leukocytes, mostly neutrophils (Fig. 4C), and experienced a severe IL-1 β , IL-6 and TNF α cytokine storm in the serum (Fig. 4D) and peritoneum (Fig. 4E). This inflammatory signature typically associates with a defect in bacterial clearance. Indeed, neutrophils from the GM/ μ MT chimeras phagocytosed bacteria poorly (Fig. 4F). The GM/ μ MT chimeras, moreover, had a modest reduction of serum IgM but not IgG (Fig. 4G), and developed severe liver and lung pathologies (Fig. 4H). Finally, bacterial titre measurements revealed that GM/ μ MT chimeras were more infected than controls (Fig. 4, I and J). Although it is possible that other bone marrow cells contribute GM-CSF for the protection against sepsis in this setting, the most likely explanation is that IRA-B cells protect against septic shock by controlling the organism's ability to clear bacteria.

GM-CSF is a pleiotropic cytokine that influences the production, maturation, function, and survival of its target cells. GM-CSF's role in sepsis has remained elusive because its indiscriminate ablation is protective (27) but its supplementation can be beneficial (28). The *in vivo* identification of GM-CSF-producing B cells illustrates a previously unrecognized locational specificity that dictates the cytokine's function. IRA-B cells differ from other subsets because their pathogen recognition pathways and tissue distribution license GM-CSF expression. The function is important in sepsis and gives rise to questions as to how IRA-B cells participate in other infectious and inflammatory diseases.

Supplementary Material

Refer to Web version on PubMed Central for supplementary material.

Acknowledgments

This work was supported in part by NIH grants 1R01HL095612 (to F.K.S.), U01 HL080731, P50 CA86355, R24 CA69246, and P01-A154904 (to R.W.). P.J.R. was supported by the Boehringer Ingelheim Fonds. C.S.R. was supported by an American Heart Association (AHA) postdoctoral fellowship. The authors thank K. Rajewsky, D. Scadden, A. Luster, and K. Otipoby (Harvard Medical School) for helpful discussions and critical reading of the manuscript. The authors thank M. Greene for secretarial assistance. The data reported in this paper are tabulated in the main paper and in the supporting online material. MIAME (minimum information about a microarray experiment)-compliant expression data have been deposited under the accession no. GSE32372.

References and Notes

1. Cohen J. The immunopathogenesis of sepsis. *Nature*. 2002; 420:885. [PubMed: 12490963]
2. Martin GS, Mannino DM, Eaton S, Moss M. The epidemiology of sepsis in the United States from 1979 through 2000. *N Engl J Med*. 2003; 348:1546. [PubMed: 12700374]
3. Hotchkiss RS, Opal S. Immunotherapy for sepsis—A new approach against an ancient foe. *N Engl J Med*. 2010; 363:87. [PubMed: 20592301]
4. Hamilton JA. Colony-stimulating factors in inflammation and autoimmunity. *Nat Rev Immunol*. 2008; 8:533. [PubMed: 18551128]
5. Materials and methods are available as supporting material on *Science* Online.

6. Sonderegger I, et al. GM-CSF mediates autoimmunity by enhancing IL-6-dependent Th17 cell development and survival. *J Exp Med*. 2008; 205:2281. [PubMed: 18779348]
7. Rittirsch D, Huber-Lang MS, Flierl MA, Ward PA. Immunodesign of experimental sepsis by cecal ligation and puncture. *Nat Protoc*. 2009; 4:31. [PubMed: 19131954]
8. Griffin DO, Rothstein TL. A small CD11b⁺ human B1 cell subpopulation stimulates T cells and is expanded in lupus. *J Exp Med*. 2011; 208:2591. [PubMed: 22110167]
9. Metcalf D, Nicola NA, Mifsud S, Di Rago L. Receptor clearance obscures the magnitude of granulocyte-macrophage colony-stimulating factor responses in mice to endotoxin or local infections. *Blood*. 1999; 93:1579. [PubMed: 10029586]
10. LeBien TW, Tedder TF. B lymphocytes: How they develop and function. *Blood*. 2008; 112:1570. [PubMed: 18725575]
11. Allman D, Pillai S. Peripheral B cell subsets. *Curr Opin Immunol*. 2008; 20:149. [PubMed: 18434123]
12. Martin F, Kearney JF. Marginal-zone B cells. *Nat Rev Immunol*. 2002; 2:323. [PubMed: 12033738]
13. Pillai S, Cariappa A. The follicular versus marginal zone B lymphocyte cell fate decision. *Nat Rev Immunol*. 2009; 9:767. [PubMed: 19855403]
14. Hao Z, Rajewsky K. Homeostasis of peripheral B cells in the absence of B cell influx from the bone marrow. *J Exp Med*. 2001; 194:1151. [PubMed: 11602643]
15. Allman D, et al. Resolution of three nonproliferative immature splenic B cell subsets reveals multiple selection points during peripheral B cell maturation. *J Immunol*. 2001; 167:6834. [PubMed: 11739500]
16. Montecino-Rodriguez E, Dorshkind K. New perspectives in B-1 B cell development and function. *Trends Immunol*. 2006; 27:428. [PubMed: 16861037]
17. Yanaba K, et al. A regulatory B cell subset with a unique CD1d^{hi}CD5⁺ phenotype controls T cell-dependent inflammatory responses. *Immunity*. 2008; 28:639. [PubMed: 18482568]
18. Ha SA, et al. Regulation of B1 cell migration by signals through Toll-like receptors. *J Exp Med*. 2006; 203:2541. [PubMed: 17060475]
19. Kawahara T, Ohdan H, Zhao G, Yang YG, Sykes M. Peritoneal cavity B cells are precursors of splenic IgM natural antibody-producing cells. *J Immunol*. 2003; 171:5406. [PubMed: 14607944]
20. Kitamura D, Roes J, Kuhn R, Rajewsky K. A B cell-deficient mouse by targeted disruption of the membrane exon of the immunoglobulin μ chain gene. *Nature*. 1991; 350:423. [PubMed: 1901381]
21. Rickert RC, Rajewsky K, Roes J. Impairment of T-cell-dependent B-cell responses and B-1 cell development in CD19-deficient mice. *Nature*. 1995; 376:352. [PubMed: 7543183]
22. Schiemann B, et al. An essential role for BAFF in the normal development of B cells through a BCMA-independent pathway. *Science*. 2001; 293:2111. [PubMed: 11509691]
23. Harris RJ, et al. Granulocyte-macrophage colony-stimulating factor as an autocrine survival factor for mature normal and malignant B lymphocytes. *J Immunol*. 2000; 164:3887. [PubMed: 10725751]
24. Mebius RE, Kraal G. Structure and function of the spleen. *Nat Rev Immunol*. 2005; 5:606. [PubMed: 16056254]
25. Lu TT, Cyster JG. Integrin-mediated long-term B cell retention in the splenic marginal zone. *Science*. 2002; 297:409. [PubMed: 12130787]
26. Doi K, Leelahavanichkul A, Yuen PS, Star RA. Animal models of sepsis and sepsis-induced kidney injury. *J Clin Invest*. 2009; 119:2868. [PubMed: 19805915]
27. Basu S, et al. Increased tolerance to endotoxin by granulocyte-macrophage colony-stimulating factor-deficient mice. *J Immunol*. 1997; 159:1412. [PubMed: 9233638]
28. Gennari R, Alexander JW, Gianotti L, Eaves-Pyles T, Hartmann S. Granulocyte macrophage colony-stimulating factor improves survival in two models of gut-derived sepsis by improving gut barrier function and modulating bacterial clearance. *Ann Surg*. 1994; 220:68. [PubMed: 8024361]
29. Bunster E, Meyer RK. An improved method of parabiosis. *Anat Rec*. 1933; 57:339.
30. Swirski FK, et al. Identification of splenic reservoir monocytes and their deployment to inflammatory sites. *Science*. 2009; 325:612. [PubMed: 19644120]

31. Colvin GA, et al. Murine marrow cellularity and the concept of stem cell competition: Geographic and quantitative determinants in stem cell biology. *Leukemia*. 2004; 18:575. [PubMed: 14749701]
32. Simon P. Q-Gene: Processing quantitative real-time RT-PCR data. *Bioinformatics*. 2003; 19:1439. [PubMed: 12874059]
33. Reich M, et al. GenePattern 2.0. *Nat Genet*. 2006; 38:500. [PubMed: 16642009]
34. Workman C, et al. A new non-linear normalization method for reducing variability in DNA microarray experiments. *Genome Biol*. 2002; 3:research0048. [PubMed: 12225587]
35. Eisen MB, Spellman PT, Brown PO, Botstein D. Cluster analysis and display of genome-wide expression patterns. *Proc Natl Acad Sci USA*. 1998; 95:14863. [PubMed: 9843981]
36. Raychaudhuri S, Stuart JM, Altman RB. Principal components analysis to summarize microarray experiments: Application to sporulation time series. *Pac Symp Biocomput*. 2000; 455

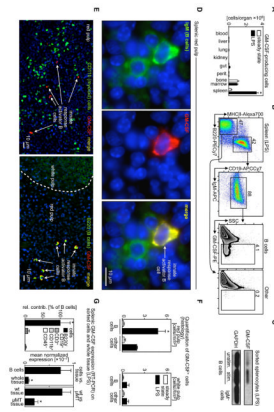


Fig. 1.

Innate response activator (IRA) B cells are GM-CSF-producing B cells that increase in number during inflammation. **(A)** Quantification of GM-CSF-producing cells retrieved from tissues in the steady state and in response to 4 daily i.p. injections of LPS (means \pm SEM, $n = 3-5$). $*P < 0.05$. **(B)** Identification of GM-CSF-producing cells in the spleen. Representative plots show percentage of B cells and their production of GM-CSF retrieved from spleens during inflammation. Data represent at least ten independent experiments. **(C)** Western blot for GM-CSF conducted on sorted cells. One of three independent experiments is shown. **(D)** Co-localization of representative GM-CSF-producing cells with IgM. **(E)** Red pulp sections with markers against CD11b (green) and GM-CSF (red) (left panel) and B220 (green) and GM-CSF (red) (right panel). Co-localization of green and red cells is yellow and the scale bar is shown in white. **(F)** Quantification of GM-CSF⁺ B cells and other cells on histological sections of the spleen in the red pulp and white pulp in the steady state and after LPS (means \pm SEM, $n = 3-4$). $*P < 0.05$. **(G)** Splenic GM-CSF expression detected by RT-PCR and conducted on sorted cells and on unprocessed spleen tissue taken from wild type and B cell knockout (μ MT) mice (means \pm SEM, $n = 3-4$). $*P < 0.05$.

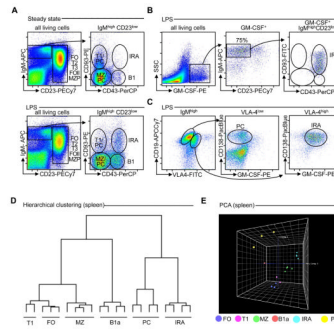


Fig. 2. IRA-B cells are a distinct subset with a unique phenotypic signature. **(A)** Flow cytometric analysis of the phenotype of IRA-B cells. Plots show B cell phenotypes retrieved from spleens during steady state and inflammation. Representative from $n > 10$ is shown. **(B)** Plots show the phenotype of GM-CSF-producing cells in the spleens during inflammation. IRA-B cells are IgM^{high} , $CD23^{low}$ $CD43^{+}$ $CD93^{+}$. **(C)** Plots show the phenotype of IRA-B cells with respect to VLA4 and CD138 expression as determined by flow cytometry. Representative from $n > 5$ is shown. **(D)** Hierarchical clustering dendrogram based on whole-genome microarray data of sorted samples of B cell subsets retrieved from LPS-treated animals and steady-state B1a. **(E)** Principal Component Analysis (PCA) of the different cell subsets shown in (D).

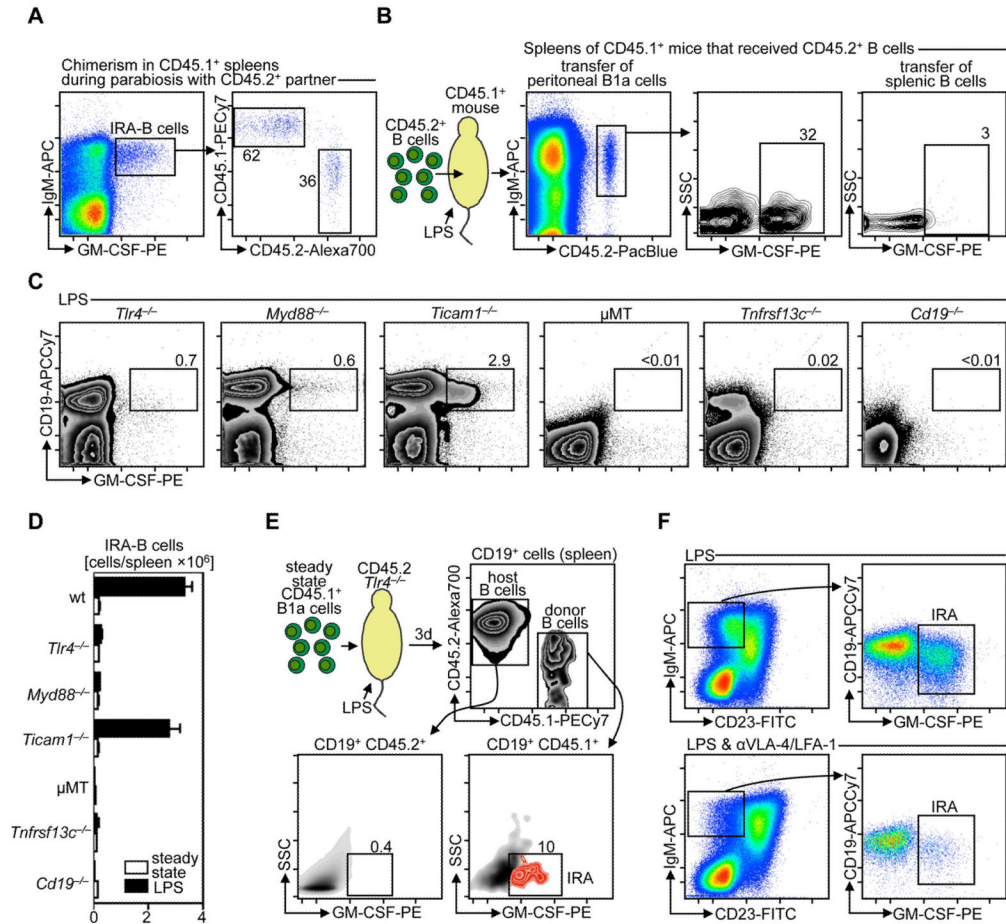


Fig. 3. IRA-B cells develop from B1a B cells via TLR4/MyD88 and reside in tissue through LFA-1/VLA-4. (A) Flow cytometric analysis of the percent chimerism is shown in spleens of CD45.1⁺ mice that had been in parabiosis with CD45.2⁺ mice for 3 weeks prior to LPS injection. Mice were sacrificed 2 days after LPS injection. Representative plots from two independent experiments are shown. (B) Adoptive transfer of peritoneal B1a B cells yields IRA-B cells. Cells from steady state CD45.2⁺ mice were transferred to CD45.1⁺ mice that then received LPS for 3 days. Animals were analyzed 72 hours after transfer. Representative plots from flow cytometric analysis of $n = 4-5$ mice are shown. (C) Flow cytometric analysis of the development of IRA-B cells in *Tlr4*^{-/-}, *Myd88*^{-/-}, *Ticam1*^{-/-} (the gene that encodes TRIF), μ MT, *Tnfrsf13c*^{-/-} (the gene that encodes BAFFR), and *Cd19*^{-/-} mice. Representative plots from $n = 4$ mice are shown. (D) Enumeration of IRA-B cells in steady state and inflammation in wt (C57BL/6) mice and in the mice shown in (D) (means \pm SEM, $n = 4-10$). * $P < 0.05$. (E) Flow cytometric analysis of the adoptive transfer of CD45.1⁺ B1a cells into congenic *Tlr4*^{-/-} CD45.2⁺ mice injected with LPS. Representative from $n = 3$ mice is shown. (F) Flow cytometric analysis of the effect of blocking VLA-4/LFA-1 on IRA-B cell retention in the spleen. Representative from $n = 3$ mice is shown.

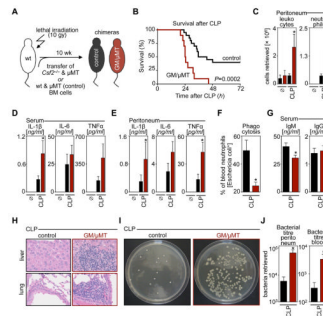


Fig. 4.

IRA-B cells protect against polymicrobial sepsis. **(A)** Generation of mixed chimeras (GM/μMT). **(B)** Kaplan-Meier curve showing survival of GM/μMT and control animals after cecal ligation and puncture (CLP). $n = 10\text{--}20/\text{group}$. **(C)** Enumeration of total leukocytes and neutrophils in the peritoneum of GM/μMT (dark red) and control (black bars) mice 20 h after CLP. **(D)** Serum levels and **(E)** peritoneal levels of inflammatory cytokines in GM/μMT (dark red) and control (black bars) mice 20 h after CLP. **(F)** Ex vivo phagocytosis assay showing capacity of neutrophils to phagocytose *E. coli* from GM/μMT (dark red) and control (black bars) mice 20 h after CLP. **(G)** serum levels of IgM and IgG 20 h after CLP in same groups as above. **(H)** Representative H&E stain of liver and lung sections 20 h after CLP in same groups as above. **(I)** Blood from GM/μMT and control mice 20 h after CLP was plated for 1 day. Representative plate shows bacterial colonies. **(J)** Enumeration of bacteremia in the peritoneum and blood of GM/μMT (dark red) and control (black bars) mice 20 h after CLP. $*P < 0.05$ [means \pm SEM, $n = 10\text{--}20/\text{group}$ for (C)–(G), (J). Four independent experiments were performed and data were grouped].